Journal of Applied Polymer Science

Understanding of intermolecular interaction in PVDF/PTW blends: Crystallization behavior, thermal, and dynamic mechanical properties

Jiajun Lu,[1] Huiyu Bai,[1,2,3] Wei Wang,[1] Shengwen Zhang,[1] Jinyuan Wang,[4] Yong Zhang,[4] Xiaoya Liu[1]

[1]The Key Laboratory of Food Colloids and Biotechnology, Ministry of Education, School of Chemical and Material Engineering, Jiangnan University, Wuxi Jiangsu 214122, China

[2]Key Laboratory of Advanced Textile Materials and Manufacturing Technology (Zhejiang Sci-Tech University), Ministry of Education, Zhejiang Sci-Tech University, Hangzhou Zhejiang 310018, China

[3]State Key Laboratory for Modification of Chemical Fibers and Polymer Materials, Donghua University, Shanghai 201620, China

[4]State Key Laboratory of Metal Matrix Composites, School of Chemistry and Chemical Engineering, Shanghai Jiao Tong University, No. 800, Dongchuan Road, Shanghai 200240, China

Correspondence to: H. Bai (E-mail: bhy.chem@163.com) and Y. Zhang (E-mail: yong_zhang@sjtu.edu.cn)

ABSTRACT: Poly(vinylidene fluoride) (PVDF)/ poly(ethylene–butylacrylate–glycidyl methacrylate) (PTW) blends were directly prepared by melt blending and the interaction and properties of PVDF/PTW blends were explored systematically. The crystallization behavior, thermal stability, dynamic mechanical property, and morphological features of PVDF/PTW blends with different ratios have been studied by XRD, attenuated total reflection Fourier transform infrared spectroscopy, differential scanning calorimeter analysis (DSC), thermal gravimetric analysis (TGA), dynamic mechanical analysis, and polarized optical microscopy (POM). The results showed that the crystalline structure of neat PVDF was dominantly α-phase crystalline and the incorporation of PTW had no effect on the crystalline structure of PVDF in the PVDF/PTW blends. And T_g of PVDF in PVDF/PTW blends shifted to higher temperature compared with that of neat PVDF, indicating the weak interaction between PVDF and PTW, which was corresponding to DSC and TGA results. An increase in the coarseness and ring-band spacing observed from POM further substantiated the weak interaction between PVDF and PTW. This work provided a way for preparing improved properties of PVDF/PTW blends for the coating material. © 2016 Wiley Periodicals, Inc. J. Appl. Polym. Sci. **2016**, *133*, 43908.

KEYWORDS: blends; properties and characterization; thermal properties; X-ray

Received 28 February 2016; accepted 10 May 2016

DOI: 10.1002/app.43908

INTRODUCTION

Polymer blending has been identified as the most effective and economic method to achieve the demand from the parent pairs.[1] Blending of polymers usually gives a new material having a good balance of properties. The utilization of polymer blends is an increasingly important segment of the plastics industry.

Poly(vinylidene fluoride) (PVDF), a semi-crystalline polymer with at least four different crystal forms: alpha, beta, gamma, and delta form,[2] has been widely studied because of its superiority in heat resistance, chemical resistance, UV resistance, mechanical properties, and electrical properties.[3,4] As a result, PVDF finds its widespread engineering applications, such as in solar back film and sensors.[5] However, PVDF also has many disadvantages, such as low surface energy, poor hydrophilicity,[6] and poor adhesion, which limit its application in a protective film.

Poly(ethylene–butylacrylate–glycidyl methacrylate) (PTW) is a crystalline polymer with epoxy groups (glycidyl) that provide with excellent adhesivity and hydrophilicity, and with butylacrylate segments that provide very good low temperature properties. The low melt viscosity of PTW also provides very good processibility. Therefore, PTW appears to be an attractive counterpart for PVDF. The chemical structure of PTW is shown in Scheme 1.

PVDF/PTW blends, with excellent balance of properties, such as excellent adhesion, favorable hydrophilicity, heat resistance, and good flow properties may be used in protective film industry.

For multicomponent blends, the miscibility between polymers has attracted much attention. The miscibility between polymers is usually related to some specific interactions between polymers, such as polar force, which can be reflected by morphology and crystallization behavior of the crystalline polymer. And the

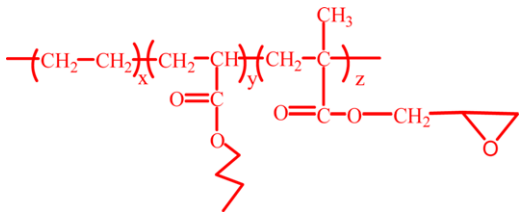

Scheme 1. Chemical structure of PTW. [Color figure can be viewed in the online issue, which is available at wileyonlinelibrary.com.]

properties of prepared polymer blends are strongly dependent on the formed phase structure[7] and interaction between blending polymers.

In recent years, miscibility and mechanical properties of PVDF/poly(methyl methacrylate) (PMMA) blends have been widely studied.[8–12] This material couple has been found to be miscible at a molecule level over the whole range in the melt because of strong dipole–dipole intermolecular interaction between carbonyl group of PMMA and the fluorines of PVDF. In addition, numerous reports about PVDF/amorphous polymer blends with carbonyl group have been published, including PVDF/poly(vinyl pyrrolidone) (PVP),[13,14] PVDF/acrylic rubber (ACM).[15–18] Otherwise, blends in which both components are crystalline polymers have received less attention compared with PVDF/amorphous systems.

In this article, systematically investigations of the interaction between PVDF and PTW were conducted. Both PVDF and PTW are crystalline polymers. And carbonyl group of PTW may provide dipole–dipole intermolecular to fluorines of PVDF. Thus, this study not only provides a fundamental investigation on properties of PVDF/crystalline polymer blends, but also suggests significant practical value of PVDF/crystalline polymer blends.

EXPERIMENTAL

Materials and Sample Preparation

The PVDF samples (trade name FR907, 3F, P. R. China) used in this work is a commercial product with the density of 1.78 g cm^{-3} and the melt index (MI) of 25 g/10 min (230 °C, 12.5 kg, ASTM D1238). The PTW (trade name Elvaloy PTW, Du Pont, USA) is a copolymer of ethylene, butyl acrylate, glycidyl methacrylate with the density of 0.94 g cm^{-3} and MI of 12 g/10 min (190 °C, 2.16 kg, ASTM D1238).

Prior to blending, PVDF and PTW were dried overnight in a vacuum oven at 80 °C and 50 °C, respectively. The PVDF/PTW blends were prepared by directly mixing the PVDF with PTW in a torque rheometer (CTR-100, Changkai scientific, China) with a twin screw at a rotation speed of 60 rpm at 200 °C for 6 min. After melt-mixing, all the blends were hot-pressed at 210 °C under 10 MPa pressure into films with the thickness of 1 mm, followed by cool-pressing at room temperature. The obtained sheets were directly used for the following characterization.

Attenuated Total Reflection Fourier Transform Infrared Spectroscopy

The crystalline structures of PVDF, PTW, and their blends were studied by Attenuated Total Reflection Fourier Transform Infrared Spectroscopy (ATR-FTIR) (Nicolet 6700, Thermo Fiaher, USA). The samples for ATR-FTIR were directly prepared by melt-press. ATR-FTIR spectra were recorded at a resolution of 2 cm^{-1} and 16 scans from 4000 to 500 cm^{-1}.

Wide-Angle X-ray Diffractometer

The wide-angle X-ray diffractometer (WAXD) (D8, Bruker, Germany) profiles were obtained by using Cu Kα radiation (40 kV, 40 mA) generated by X-ray diffractometer with a scanning speed of 1°/cm from 2θ = 5–30°.

Differential Scanning Calorimeter Analysis

Differential scanning calorimeter analysis (DSC) (DSC-8000, Perkin–Elmer, USA) was used to investigate the crystallization and melting behavior of all the samples. The experiment was conducted under high pure nitrogen atmosphere. Before samples scan, the differential scanning calorimeter was calibrated with the melting temperature of indium and zinc. The samples were first heated to 200 °C and held for 5 min to eliminate the thermal history. The samples were then cooled down to 0 °C and held for 5 min, followed by heated to 200 °C. Both the cooling and heating rates were 10 °C/min and the first cooling and second heating data were recorded. All the DSC curves were normalized by sample weight after a baseline correction.

Thermal Gravimetric Analysis

Thermal gravimetric analysis (TGA) (1100SF, Mettler-Toledo International Trade, Switzerland) was used to evaluate the thermal stability of the samples. The experiment was performed under nitrogen atmosphere. The temperature increased from room temperature to 600 °C at a heating rate of 20 K/min.

Dynamic Mechanical Analysis

Dynamic mechanical analysis (DMA) (STARe SW 10.00, Mettler-Toledo International Trade, Switzerland) was carried out in tensile-film mode. The samples (9 × 3 × 1 mm^3) were tested under a nitrogen atmosphere from −140 °C to 150 °C. The frequency and heating rate were set as 1 Hz and 3 °C/min, respectively.

Polarized Optical Microscopy

Morphological observations on crystallites of PVDF and PVDF/PTW blends were conducted on Polarized optical microscopy (POM) (Leica DMLP, Germany) equipped with a hot stage under crossed polarizers. All samples were first inserted between two microscope cover slips and squeezed at 200 °C to obtain a slice with a thickness around 30 μm. Subsequently, the as-prepared slice was transferred to the hot stage and held at 200 °C for 5 min to achieve thermal equilibrium. It was followed by cooling to 158 °C at 100 °C/min and isothermally crystallized at 158 °C. The POM micrographs were recorded by a digital camera.

RESULTS AND DISCUSSION

Crystalline Structure of PVDF and FTIR Analysis

Figure 1 showed XRD patterns of neat PVDF, neat PTW, and their blends. PTW was a polymer with low crystallinity. As shown in Figure 1, a large and broad halo, which originated from the amorphous region of PTW and small and broad diffraction peaks, which were because of the low crystallinity of PTW were observed. PVDF was a semi-crystalline polymer and exhibited polymorphism. The most common polymorph was nonpolar α-phase and it can be generally produced by melt blending.[19] As shown in Figure 1, neat PVDF showed four characteristic diffraction peaks

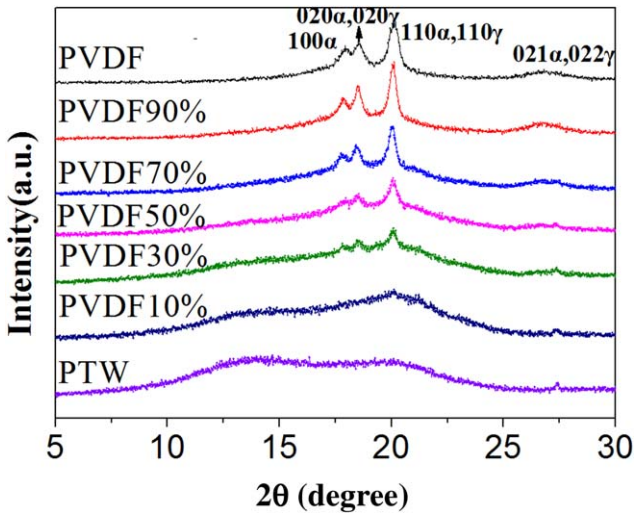

Figure 1. XRD patterns of neat PVDF, PTW and their blends. [Color figure can be viewed in the online issue, which is available at wileyonlinelibrary.com.]

at 17.8°, 18.5°, 20.0°, and 26.7°, which was appointed to the (100), (020), and (021) reflections of the α-phase crystalline,[20] indicating the dominant α-phase crystalline in neat PVDF. And no typical peaks of β-phase crystalline were observed from the XRD pattern. However, it has been reported that γ-phase crystalline PVDF has the similar XRD profile to the ones of α-phase crystalline PVDF, which γ (020), γ (110), and γ (022) maybe overlapped with the α (020), α (110), and α (021) respectively.[21] So it was difficult to decide whether the neat PVDF had γ-phase crystalline only from XRD pattern. As shown in Figure 1, with the incorporation of PTW, α-phase diffraction peak of PVDF could also be observed and no typical β-phase existed, which was similar to that of neat PVDF, indicating that crystalline structure of PVDF in the PVDF/PTW blends was not affected by PTW.

In order to further study whether γ-phase crystalline form of PVDF in neat PVDF and PVDF/PTW blends existed or not, ATR-FTIR was carried out and the results were shown in Figure 2. As

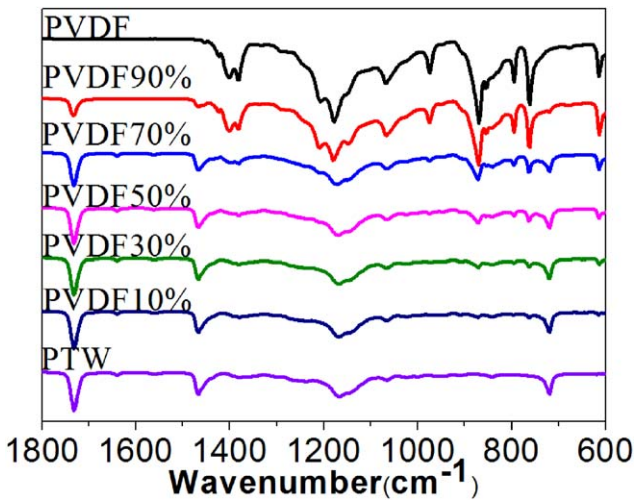

Figure 2. ATR-FTIR spectra of neat PVDF, PTW and their blends. [Color figure can be viewed in the online issue, which is available at wileyonlinelibrary.com.]

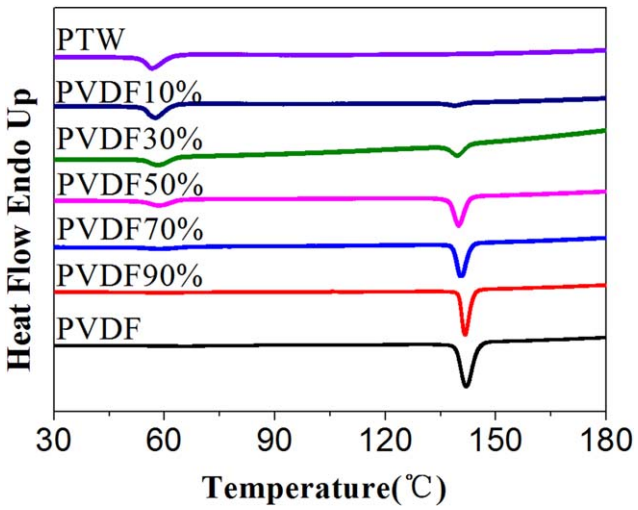

Figure 3. DSC thermograms during cooling for PVDF, PTW and their blends. [Color figure can be viewed in the online issue, which is available at wileyonlinelibrary.com.]

shown in Figure 2, the absorption peaks at 615, 764, 796, 855, 976, and 1385 cm^{-1}, which were typical absorption of α-phase crystalline,[22] were observed while the absorption peaks at 1275, 1232 cm^{-1} were not found in PVDF and PVDF/PTW blends. It has been reported that the β-phase crystalline showed typical absorption at 1275cm^{-1} and γ-phase crystalline absorption at 1232cm^{-1}.[23,24] These facts indicated the polymorph of PVDF in neat PVDF and PVDF/PTW blends was α-phase and the incorporation of PTW had less effect on the crystalline structure of PVDF in the PVDF/PTW blends which was because of the weak intermolecular interaction between PVDF and PTW in the PVDF/PTW blends.

From Figure 2, it was clear to see that the absorption peak of carbonyl group in the PVDF/PTW blends has been almost unchanged, revealing that the interaction between $–CF_2$ of PVDF and carbonyl group of PTW was weak. Bernstein *et al.*[8]

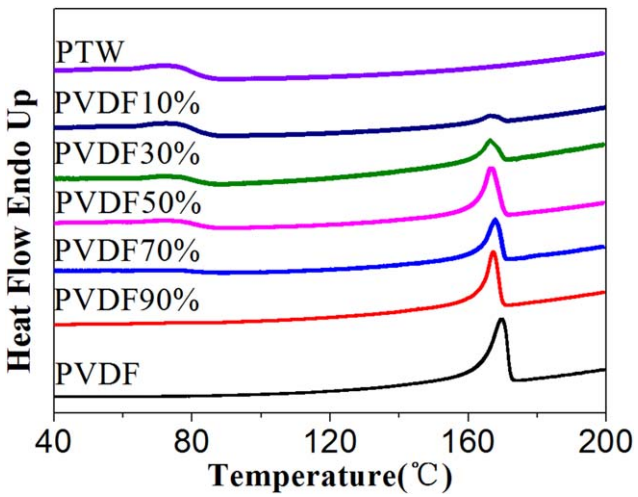

Figure 4. DSC thermograms during heating for PVDF, PTW and their blends. [Color figure can be viewed in the online issue, which is available at wileyonlinelibrary.com.]

Table I. Crystallinity of PVDF in PVDF/PTW Blends

Component	PVDF	PVDF 90%	PVDF 70%	PVDF 50%	PVDF 30%	PVDF 10%	PTW
Crystallinity of PVDF (%)	40.1	39.6	37.2	36.7	36.5	30.0	—
Relative Crystallinity of PTW (%)	—	113.2	110.4	108.6	105.4	102.5	100

reported that PVDF and PMMA can be miscible at a molecular level over the whole composition range in the melt below a lower critical solution temperature (LCST) of 350 °C because of strong dipole–dipole intermolecular interactions between the carbonyl group of PMMA and the fluorines of PVDF. In our work, for PVDF/PTW blends, the miscibility between PVDF and PTW was related to weak dipole–dipole intermolecular interactions between PTW and PVDF. Thus, PVDF and PTW could not be miscible at a molecular level over the whole composition range and they were partially miscible in some PVDF/PTW blends.

Crystallization and Melting Behavior of PVDF/PTW Blends

The crystallization and melting behavior of PVDF/PTW blends were examined by using DSC. Figure 3 showed the DSC cooling curves of the samples at 10 °C/min from melting. As shown in Figure 3, it was clear to see that the crystallization peak temperature (T_c) of PVDF in the blends decreased with the increasing the content of PTW. This meant that the existence of PTW impeded the crystallization of PVDF. In partial miscible and miscible blend system, the both components would affect each other during crystallization. This phenomenon has been reported in many miscible systems, such as PVDF/poly(butylene succinate) (PBS) blends.[25] The difference in T_c of the PVDF and PTW was relatively large, so two-step crystallization usually occurred, in which the high-T_c component (PVDF) crystallized first during cooling from melt, at the same time, the other component (PTW) was still in a molten state. Thus, the molten PTW acted as diluting agent for PVDF and a long migrating distance was needed from the melt to the lattice for the PVDF chain during crystallization, consequently, the lower crystallization temperatures of the blends were observed with the addition of PTW (see Figure 3).Conversely, crystallized PVDF acted as nucleating agent for PTW and promoted the crystallization rate for PTW. Therefore, crystallization peak of PTW in PVDF/PTW blends moved to higher temperature than the neat PTW (see Figure 3). These results also indicated the interaction between PVDF and PTW in the PVDF/PTW blends existed.

The second heating curves following the cooling process have been presented in Figure 4. As shown in Figure 4, the decrease in the melting temperatures of the PVDF in the PVDF/PTW blends comparing with that of neat PVDF, providing important information about the interaction between PVDF and PTW in the crystalline region, which the depression of the chemical potential of the PVDF was because of the addition of PTW. And it was reported that the most of miscible polymer blends containing crystalline components showed the melting point depression because of the thermodynamic interaction between the component polymers in the crystalline regions.[26,27]

The crystallinity of PVDF and relative crystallinity of PTW (it was hard to find the melting enthalpy when crystallinity of PTW was 100%, so it was considered that the crystallinity of neat PTW was 100%) were calculated as below:

$$X_c = \frac{\Delta H_m}{\varphi \times \Delta H_m^*} \times 100\% \quad (1)$$

where ΔH_m was the melting enthalpy of samples measured from the second melting curves, ΔH_m^* was the melting enthalpy when the crystallinity of the polymer was 100% (as for PTW in the blends, ΔH_m^* was the melting enthalpy of neat PTW) and φ was the mass fraction of PVDF or PTW in the blends.

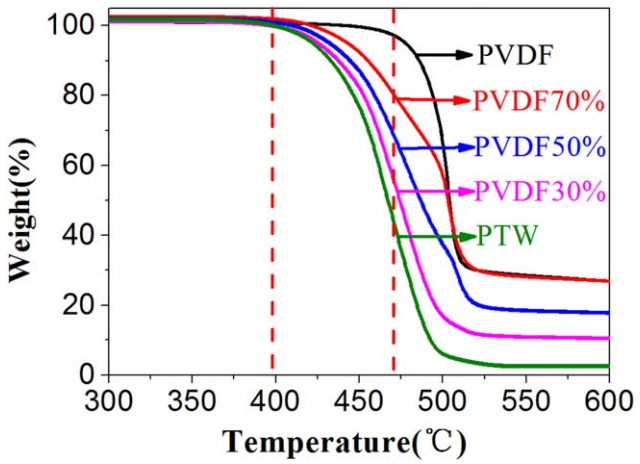

Figure 5. TGA curve for PVDF, PTW and their blends. [Color figure can be viewed in the online issue, which is available at wileyonlinelibrary.com.]

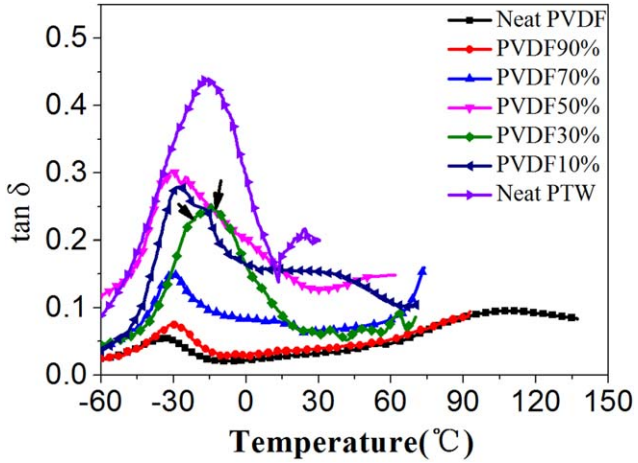

Figure 6. Tan δ as a function of temperature for PVDF, PTW and their blends. [Color figure can be viewed in the online issue, which is available at wileyonlinelibrary.com.]

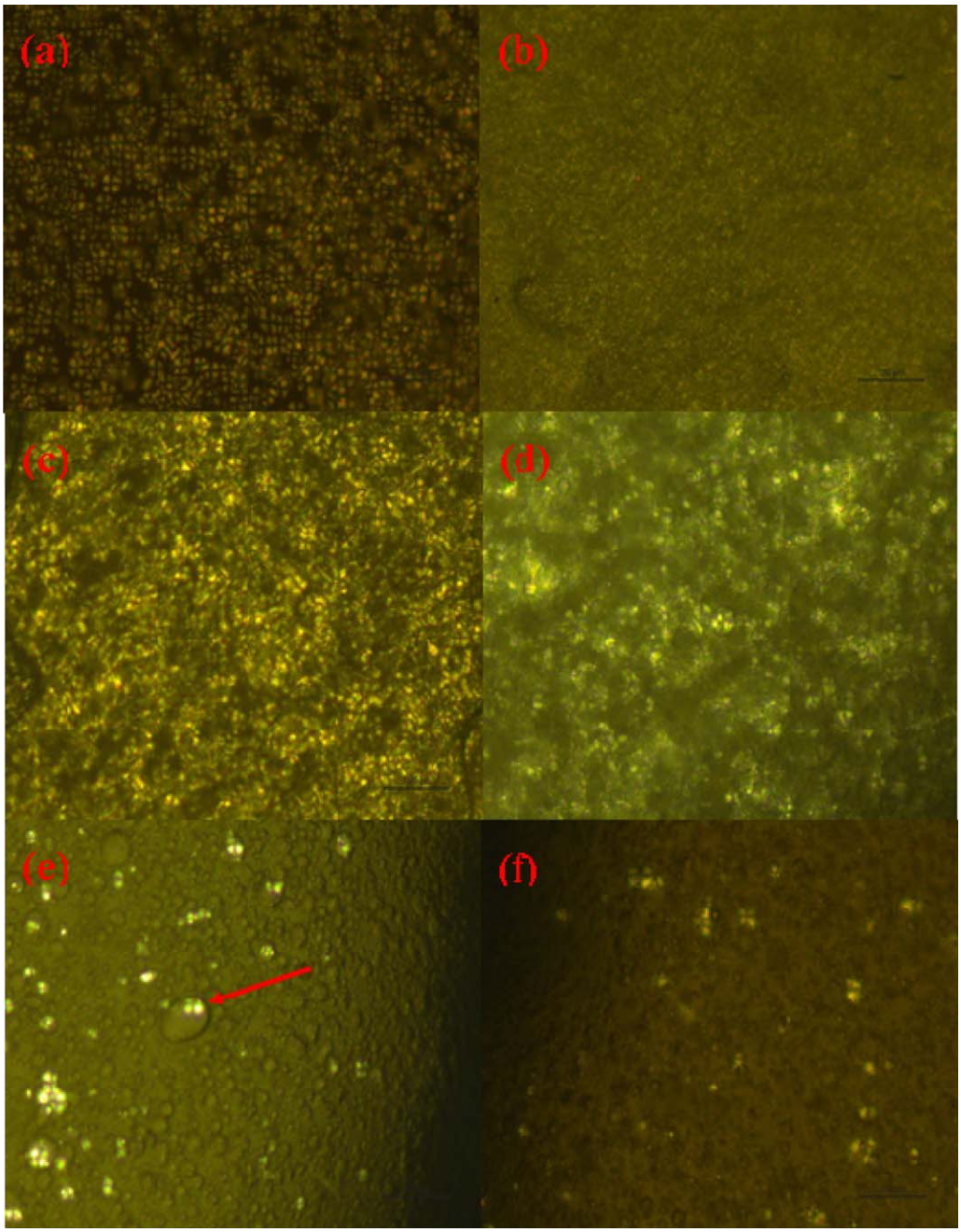

Figure 7. Ring-band spherulites under POM in neat PVDF (a,a'), PVDF90% (b,b'), PVDF 70% (c,c'), PVDF 50% (d,d'), PVDF 30% (e,e') and PVDF 10% (f,f') blends [the scale bar of (a,b,c,d,e,f) was 100 μm; the scale bar of (a',b',c',d',e',f') was 50 μm]. [Color figure can be viewed in the online issue, which is available at wileyonlinelibrary.com.]

The detailed parameters were listed in Table I. As shown in Table I, compared with the crystallinity of neat PVDF ($X_c = 40.1\%$), the incorporation of PTW induced the decrease in the crystallinity of PVDF and as the content of PTW in PVDF/PTW blends increased, the crystallinity of PVDF in the blends deceased. On the other hand, the crystallized PVDF acted as nucleating agent for PTW and promoted the increasing crystallinity of PTW as the content of PVDF increased.

Therefore, PTW not only induced the depression of the crystallization and melting temperature of PVDF, but also induced the decrease in the crystallinity of PVDF. Conversely, the PVDF not only promoted to increase the crystallization and melting temperature of PTW, but also induced the increase in the crystallinity of PTW. These facts also indicated the weak interaction between PVDF and PTW in the PVDF/PTW blends.

Thermal Stability of PVDF/PTW Blends

The thermal stability of PVDF, PTW, and their blends was evaluated by using TGA in the nitrogen atmosphere, as shown in Figure 5. For clarity purpose, the curves of PVDF 90% and PVDF 10% were not shown in Figure 5. As shown in Figure 5,

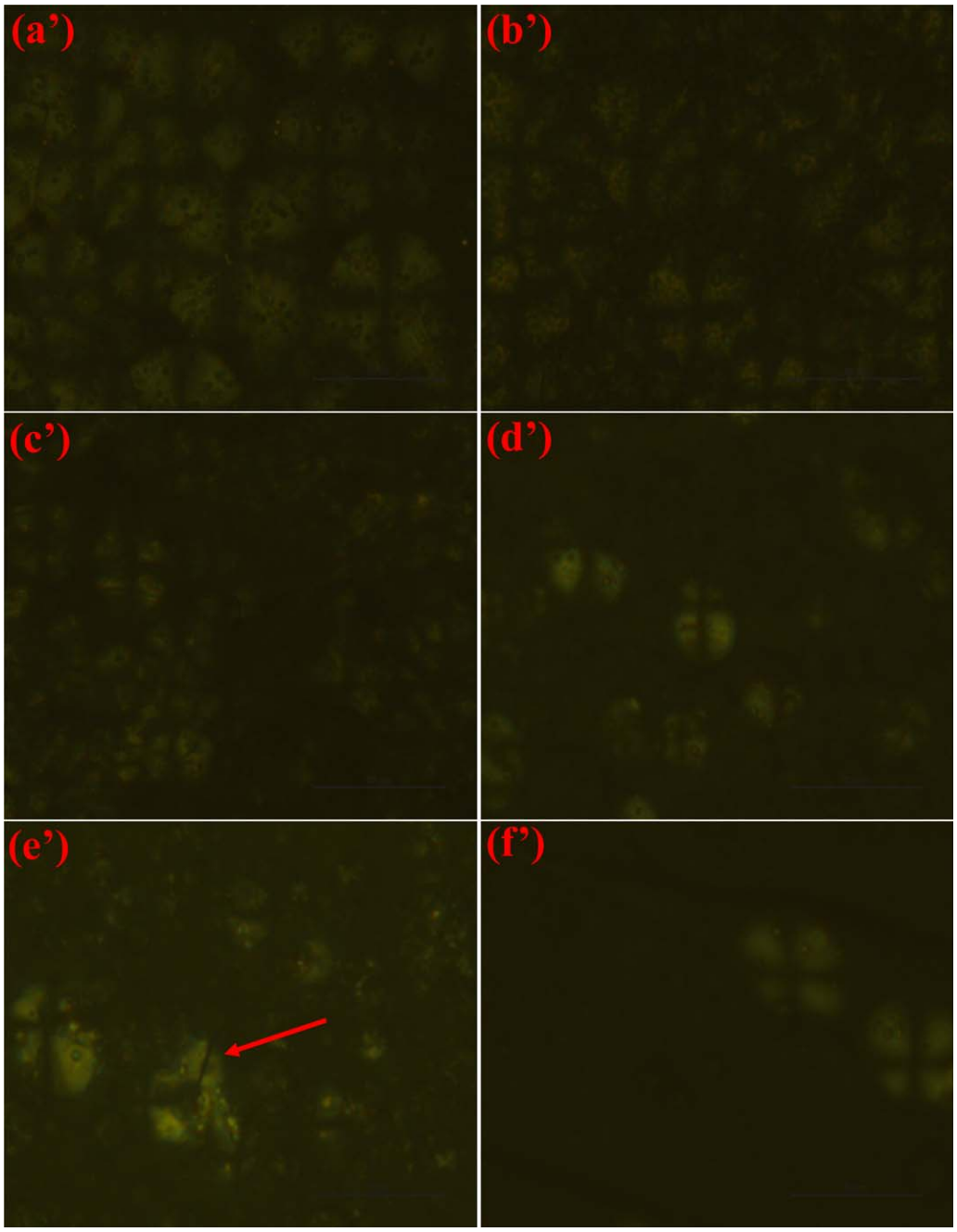

Figure 7. (*Continued*). [Color figure can be viewed in the online issue, which is available at wileyonlinelibrary.com.]

both neat PVDF and PTW showed the typical single degradation step profile. The main PVDF degradation occurred between 435 °C and 537 °C and the main PTW degradation occurred between 370 °C and 520 °C, indicating that both PVDF and PTW had good thermal stability. It was clear to see from Figure 5 that incorporation of PTW component reduced the thermal stability of the PVDF/PTW blends to a certain extent, compared with neat PVDF. From the region between the two dotted lines (the temperature between the onset decomposition temperature of PTW and that of PVDF) in Figure 5, the decomposition curves for PVDF/PTW blends with different contents of PTW moved to higher temperatures compared with that of neat PTW, indicating that the interaction between PVDF and PTW existed.

Dynamic Mechanical Properties Analysis

In order to investigate the weak interaction between PVDF and PTW, DMA was carried out to detect segment relaxation for neat PVDF, PTW, and their blends. Dynamic mechanical properties were proven to be a useful way to investigate phase evolution in partially miscible blends thanks to their sensitive to phase change.[28,29] The evaluation included the glass transition

temperature (T_g) of the polymers intimately was related to the intermolecular interaction of PVDF and PTW. Figure 6 showed the plot of tan δ as a function of temperature for PVDF, PTW, and their blends. As shown in Figure 6, for neat PVDF, two relaxations were observed. A sharp relaxation peak at about −35 °C was corresponding to the motion of molecular segments in amorphous region and the relaxation at high temperature (about 100 °C) was considered to be α-relaxation (imperfection in crystalline PVDF phase). The relaxation peak at about 37 °C, at which the γ′ relaxation corresponding to the movement of the molecular chains at the amorphous–crystal interface[28,30,31] was reported to occur, was not observed. That was consistent with the results of XRD and ATR-FTIR. For neat PTW, a very broad relaxation peak at about −16.6 °C was observed because of its low crystallinity, which was corresponding to the T_g of PTW.

For the blends with more than 70 wt % PVDF, only one T_g can be detected, indicating the good miscibility between amorphous part of PTW and the amorphous part of PVDF. In contrast, although the T_g of neat PVDF and PTW was very close, one can observe two shoulders of the blends with 50%, 30%, 10% wt PVDF, indicating partial miscibility between PVDF and PTW when PVDF was less than 70 wt %, as shown in Figure 6. The fact that two T_gs were observed revealing that two-phase structure for the blends when PVDF content was less than 70 wt %. It was considered that the two phases were PVDF-rich phase and PTW-rich phase, respectively. Moreover, the T_g of PVDF in PVDF/PTW blends showed a little shift to higher temperature compared with that of neat PVDF, indicating weak interaction between PVDF and PTW in PVDF/PTW blends. In our previous work, we have prepared PVDF/PTW blends prepared directly by melt blending and the principle of time-temperature superposition (t*TS*) was used to confirm the miscibility between PVDF and PTW and found that when the content of PTW is 10 wt %, t*TS* worked well and PVDF had good miscibility with PTW and with the increase in the amount of PTW in PVDF/PTW blends, the viscoelastic properties of PVDF/PTW blends were different from characteristic thermorheological responses, especially for the characteristic deviations of the storage modulus at low frequencies corresponding to the homogeneous system. These facts indicated the worse miscibility between PVDF and PTW with increasing amount of PTW in PVDF/PTW blends. This result was also proven by SEM images.[32]

Spherulite Patterns of PVDF/PTW Blends

Figure 7 showed POM graphs with enlarged spherulites of neat PVDF and PVDF/PTW blends. As shown in Figure 7, neat PVDF (a,a') displayed fine ring bands, which could be observed under high isothermal crystalline temperature and large enough magnification under POM. From POM, patterns and inter-band spacing of PVDF/PTW blends was found to be different to that of neat PVDF. The band width of PVDF of PVDF/PTW blends (b,b'; c,c'; d,d'; e,e'; f,f') became smaller compared with neat PVDF. With the increasing PTW contents in PVDF/PTW blends, the ring band of PVDF was disrupted or distorted and became unclear while the concentric rings were coarser and paced with a greater distance, indicated by arrow in Figure 7(e,e'). These results were because of the fact that the molten PTW restrained the crystallization of PVDF, which was corresponding with DSC results. An increasing in coarseness and band spacing provided supportive evidence that miscibility exists between PVDF and PTW in the blend.[33] And pattern changes in ring-band spherulites of the blends further demonstrated the favorable interaction between PVDF and PTW constituents.

CONCLUSIONS

In our study, the intermolecular interaction between PVDF and PTW was systematically studied. The results showed that PVDF/PTW blends exhibited boardline miscibility with weak interaction. From XRD patterns and ATR-FTIR spectra, it was found that the crystalline structure of neat PVDF was dominant α-phase crystalline and incorporation of PTW had less effect on the crystalline structure of PVDF. From DSC analysis, compared with that of the neat PVDF, the melting temperatures of PVDF in the PVDF/PTW blends decreased, providing important information about the interaction between PVDF and PTW in the crystalline region. From TGA, the decomposition curves for PVDF/PTW blends moved to higher temperature compared with that of neat PTW, indicating that the interaction between PVDF and PTW did exist. From the DMA analysis, the T_g of PVDF in PVDF/PTW blends showed a little shift to higher temperature compared with that of neat PVDF, indicating the weak interaction between PVDF and PTW in the amorphous region. From POM, an increase in both coarseness and band spacing was observed, which provided supportive evidence that miscibility existed between PVDF and PTW. In addition, the thermodynamics of intermolecular interaction may appear to be an important effect on the interaction in PVDF/PTW blends. In-depth studies on the thermodynamic of intermolecular interaction between PVDF and PTW in PVDF/PTW blends and the type of intermolecular interaction should be performed in order to shed more light on the understanding of the intermolecular interaction in PVDF/PTW blends.

ACKNOWLEDGMENTS

This work was supported by State Key Laboratory for Modification of Chemical Fibers and Polymer Materials, Donghua University (LK 1426) and Key Laboratory of Advanced Textile Materials and Manufacturing Technology (Zhejiang Sci-Tech University), Ministry of Education (2014003) and Cooperative Innovation Fund (BY2014023-07). The authors also acknowledge Dr. Weixia Zhong for her help in DMA experiment.

REFERENCES

1. Wang, T. C.; Li, H. H.; Wang, F.; Schultz, J. M.; Yan, S. K. *Polym. Chem.* **2011**, *2*, 1688.
2. Lovinger, A. *J. Macromolecules* **1982**, *15*, 40.
3. Furukawa, T. *IEEE. Trans. Electr. Insul.* **1989**, *24*, 375.
4. Koga, K.; Ohigashi, H. *J. Appl. Phys.* **1986**, *59*, 2142.
5. Chen, Q. X.; Payne, P. A. *Meas. Sci. Technol.* **1995**, *6*, 249.
6. Lang, M. H.; Zhang, J. *Iran. Polym. J.* **2013**, *22*, 821.

7. Lang, M. H.; Zhang, J. *Plast. Rubber. Compos.* **2014**, *43*, 8.
8. Bernstein, R. E.; Cruz, C. A.; Paul, D. R.; Barlow, J. W. *Macromolecules* **1977**, *10*, 681.
9. Nishi, T.; Wang, T. T. *Macromolecules* **1975**, *8*, 909.
10. Paul, D. R.; Altamirano, J. O. *Adv. Chem. Ser.* **1975**, *142*, 371.
11. Mijović, J.; Luo, H. L.; Han, C. D. *Polym. Eng. Sci.* **1982**, *22*, 234.
12. Zhang, H. G.; Lamnawar, K.; Maazouz, A. *Macromolecules* **2012**, *46*, 276.
13. Cheng, J.; Wang, S. C.; Chen, S. J.; Zhang, J.; Wang, X. L. *Polym. Int.* **2012**, *61*, 477.
14. Chen, N. P.; Hong, L. *Polymer* **2002**, *43*, 1429.
15. Li, Y. J.; Iwakura, Y.; Zhao, L.; Shimizu, H. *Macromolecules* **2008**, *41*, 3120.
16. Li, Y. J.; Iwakura, Y.; Shimizu, H. *Macromolecules* **2008**, *41*, 3396.
17. Li, Y. J.; Oono, Y.; Nakayama, K.; Shimizu, H.; Inoue, T. *Polymer* **2006**, *47*, 3946.
18. Li, Y. J.; Oono, Y.; Kadowaki, Y.; Inoue, T.; Nakayama, K.; Shimizu, H. *Macromolecules* **2006**, *39*, 4195.
19. Xing, C. Y.; Zhao, M. M.; Zhao, L. P.; You, J. C.; Cao, X. J.; Li, Y. *J. Polym. Chem.* **2013**, *4*, 5726.
20. Gregorio, R. *J. Appl. Polym. Sci.* **2006**, *100*, 3272.
21. Ince-Gunduz, B. S.; Alpern, R.; Amare, D.; Crawford, J.; Dolan, B.; Jones, S.; Kobylarz, R.; Reveley, M.; Cebe, P. *Polymer* **2010**, *51*, 1485.
22. Yee, W. A.; Kotaki, M.; Liu, Y.; Lu, H. X. *Polymer* **2007**, *48*, 512.
23. Gregorio, R. Jr.; Cestari, M. *J. Polym. Sci. Part B: Polym. Phys.* **1994**, *32*, 859.
24. Kim, K. J.; Cho, Y. J.; Kim, Y. H. *Vib. Spectrosc.* **1995**, *9*, 147.
25. Lee, J. C.; Tazawa, H.; Ikehara, T.; Nishi, T. *Polym. J.* **1998**, *30*, 327.
26. Paul, D. R.; Newman, S. In Polymer Blend; Academic Press: New York, **1978**
27. Shonaike, G. O.; Simon, G. P. In Polymer Blends and Alloys; Marcel Dekker: New York, **1999;** Vol *1*.
28. Liu, Z. H.; Marechal, P.; Jerome, R. *Polymer* **1997**, *38*, 4925.
29. Linares, A.; Acosta, J. L. *Eur. Polym. J.* **1997**, *33*, 467.
30. Mandal, A.; Nandi, A. K. *J. Mater. Chem.* **2011**, *21*, 15752.
31. Manna, S.; Batabyal, S. K.; Nandi, A. K. *J. Phys. Chem. B* **2006**, *110*, 12318.
32. Lu, J. J.; Bai, H. Y.; Wang, W.; Liu, J.; Ma, P. M.; Dong, W. F.; Liu, X. Y. *Acta Polym. Sin.* **2016**, to appear.
33. Li, S. H.; Woo, E. M. *J. Appl. Polym. Sci.* **2008**, *107*, 766.